

Bootstrapping the Four-Point NMHV Stress-Tensor Form Factor

Song He (何颂)^{1,2,*} Jiahao Liu (刘家昊)^{1,3,†} and Qinglin Yang (杨清霖)^{4,‡}

¹*New Cornerstone Laboratory, Institute of Theoretical Physics,
Chinese Academy of Sciences, Beijing 100190, China*

²*School of Fundamental Physics and Mathematical Sciences,*

Hangzhou Institute for Advanced Study, UCAS & ICTP-AP, Hangzhou, 310024, China

³*School of Physical Sciences, University of Chinese Academy of Sciences, No. 19A Yuquan Road, Beijing 100049, China*

⁴*Max Planck Institut für Physik, Werner Heisenberg Institut, D85748 Garching bei München, Germany*

We bootstrap the two-loop four-point next-to-maximally helicity-violating (NMHV) ratio function for the chiral stress-tensor form factor in planar maximally supersymmetric Yang-Mills theory (sYM) at the symbol level. Starting from an ansatz built from NMHV leading singularities and the known two-loop five-point one-mass integral function space, we impose finiteness, dihedral symmetry, parity and Galois symmetry, spurious-pole cancellation, collinear limits, and finally triple-collinear consistency, which together fix the result uniquely. We then subject the answer to independent soft and double-soft checks. The resulting symbol contains 78 letters, all drawn from the 88-letter alphabet previously identified for the four-point MHV form factor through four loops. This provides the first multi-loop result for a non-MHV form factor, and direct evidence that the 88-letter alphabet extends beyond the MHV sector, which may provide the natural universal alphabet for four-point form factors. Our result supplies new data for the study of physics and mathematics of multi-loop form factors including the antipodal duality, as well as their relations to Higgs-parton amplitudes in QCD.

INTRODUCTION

Gluon fusion is the dominant production mechanism for Higgs bosons at colliders. Consequently, the corresponding scattering amplitudes are key observables for testing the Standard Model and probing new physics. In the large-top-mass limit, Higgs-plus-parton amplitudes can be reduced to form factors of gauge-invariant effective operators [1, 2], making the analytic calculation and investigation of form factors an essential component of particle-physics studies.

In modern scattering-amplitude research, supersymmetric form factors of the chiral stress-tensor supermultiplet [3] (half-BPS form factors) in planar maximally supersymmetric Yang-Mills theory ($\mathcal{N}=4$ sYM) have become a useful counterpart of the Higgs-production form factor; see the recent review [4]. Many methods and ideas originally developed for scattering amplitudes in $\mathcal{N}=4$ sYM can be applied to form factors with suitable modifications. These include the form factor/periodic Wilson-loop duality [5–9], which is used to compute two-loop MHV form factors at all multiplicities [10], recursion relations for tree-level objects and loop integrands [11], Grassmannian geometry and on-shell diagrams for leading singularities [12–14], color-kinematics duality [15–18], the form factor operator product expansion (OPE) [19–22], and the Steinmann/cluster bootstrap program (see the review [23]). For form factors of the stress-tensor supermultiplet, or equivalently the half-BPS $\text{Tr}(\phi^2)$ multiplet, this bootstrap program has been used to compute the three-point MHV form factor up to eight loops and the four-point MHV form factor up to four loops [24–29]. Related three-point MHV form factor for the $\text{Tr}(\phi^3)$ op-

erator has been calculated to six loops [30, 31]; see also [32] for the two-loop four-point case.

Similar to scattering amplitudes in $\mathcal{N} = 4$ sYM, half-BPS form factors have been found to exhibit a variety of simplifications, hidden symmetries and structures. At tree level and one loop, they have been shown to possess a dual conformal invariance structure [33]. At higher perturbative orders, the three-point MHV form factor is organized by a C_2 -type cluster algebra, while the four-point MHV alphabet up to four loops is controlled by 88 symbol letters. More strikingly, the three-point MHV form factor was found to be antipodally dual to the six-point MHV amplitude [34, 35]. A closely related antipodal self-duality was later uncovered in the four-point MHV form factor [25], offering an explanation for the three-point duality. Finally, it was found in [36–38] that three-point MHV form factors coincide with the maximally transcendental parts of $H \rightarrow ggg$ amplitudes, providing another important example of the principle of maximal transcendentality between $\mathcal{N}=4$ sYM and QCD [39–41]. The study of half-BPS form factors is therefore expected to reveal, in a controlled setting, deeper mathematical and physical structures underlying collider processes involving Higgs production.

In this work, we extend the bootstrap study of form factors of the stress-tensor supermultiplet beyond the MHV sector by bootstrapping the ratio function of the four-point NMHV form factor at two loops, first at symbol level [42, 43]. Beyond MHV, one encounters non-trivial leading-singularity prefactors and a richer set of physical constraints and limits. We organize the ansatz in terms of three classes of form-factor leading singularities as kinematic prefactors. Instead of constructing all integrable symbols directly from the 113 letters of

the two-loop one-mass master integrals, we build on the known five-point one-mass function space [44–47] constructed by the canonical differential equation (CDE) method [48, 49]. We then impose physical consistency conditions to fix the result and subject it to independent checks. The final symbol contains 78 letters, all drawn from the 88-letter alphabet of the four-point MHV form factor. Our result strongly suggests that, the NMHV form factors possess a decomposition structure of definite leading singularities at all-loop order, marking a first step toward the explicit calculation of higher-loop quantities and further exploration of its underlying mathematical structure.

NMHV FORM FACTOR RATIO FUNCTION AND LEADING SINGULARITIES

We consider the four-point super form factor in the large- N_c limit [8, 50],

$$\mathcal{F}_4(p_i, q, \eta_i) := \int d^4x d^4\theta^+ e^{-i(qx + \theta^+ \gamma)} \langle \Omega_4 | \mathcal{T}(x, \theta^+) | 0 \rangle \quad (1)$$

where the chiral stress-tensor multiplet is $\mathcal{T}(x, \theta^+) = \text{Tr}(\phi(x)^2) + \dots + (\theta^+)^4 \mathcal{L}(x)$, with $\mathcal{L}(x)$ denoting the chiral on-shell Lagrangian of $\mathcal{N} = 4$ sYM, and $\langle \Omega_4 |$ is the four-particle external superstate depending on $\{p_i, \eta_i\}$. This quantity has a natural decomposition [8, 51]

$$\mathcal{F}_4 = \mathcal{F}_{4,0} + \mathcal{F}_{4,1} + \mathcal{F}_{4,2}, \quad (2)$$

where $\mathcal{F}_{4,k}$ has Grassmann degree $4k + 8$. The MHV sector $\mathcal{F}_{4,0}$ has been studied previously in the bootstrap literature [25] and has recently been extended to four loops [29]. We define the ratio function by

$$\mathcal{F}_{4,1} = \mathcal{F}_{4,0} \mathcal{R}_4. \quad (3)$$

Our goal is to determine (the symbol of) the infrared-finite two-loop ratio function $\mathcal{R}_4^{(2)}$.

The kinematics of $\mathcal{F}_{4,1}$ depends on four massless external legs p_i and one off-shell operator momentum, $q = \sum_{i=1}^4 p_i$, with $p_i^2 = 0$ and $q^2 \neq 0$. We use the eight dimensionless invariants [25]

$$u_i = \frac{(p_i + p_{i+1})^2}{q^2}, \quad v_i = \frac{(p_i + p_{i+1} + p_{i+2})^2}{q^2}, \quad (4)$$

with $1 \leq i \leq 4$, which obey three independent linear relations: $-u_1 + u_3 + v_4 + v_1 = 1$ together with two independent cyclic images; these leave five independent kinematic variables. In practice, we implement the kinematics using periodic momentum twistors and an OPE parametrization [19–22]; we refer to the Supplemental Material for explicit parametrizations used here.

Similar to superamplitudes in $\mathcal{N}=4$ sYM, supersymmetric form factors at L loops admit a decomposition

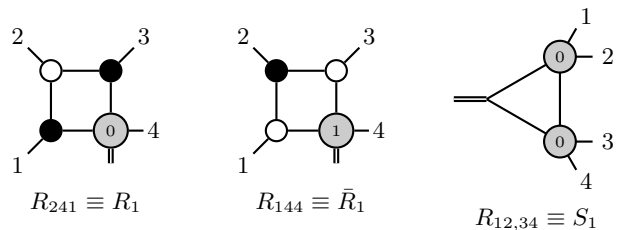


FIG. 1: Representatives for four-point form factor leading singularities. Black/white trivalent vertices denote three-point MHV/ $\overline{\text{MHV}}$ superamplitudes, respectively. Gray blobs denote form-factor/amplitude vertices; the integer inside each blob labels its N^k MHV degree k . A double line marks the off-shell momentum carried by the operator insertion.

into products of supersymmetric kinematic prefactors, known as *leading singularities* or *R-invariants* [52–54], and weight- $2L$ bosonic transcendental functions. Already at one loop, the four-point NMHV form factor involves three types of leading singularities [33, 50]: the two box-type *R*-invariants $R_1 = R_{241}$ and $\bar{R}_1 = R_{144}$, together with the algebraic *R*-invariant $S_1 = R_{12,34}$. They can be computed from supersymmetric on-shell diagrams, constructed by gluing tree-level amplitudes and form factors, as shown in Fig. 1. The prefactor \bar{R}_1 is drawn in a different but equivalent on-shell representation compared to Ref. [33], making its parity relation to R_1 manifest. In addition, form factors admit algebraic prefactors such as S_1 from a three-mass-triangle maximal cut, absent for sYM NMHV amplitudes. We provide more details about these leading singularities and their expressions in terms of momentum twistors in the Supplemental Material.

Motivated by the on-shell-diagram construction and the Grassmannian interpretation of supersymmetric on-shell functions [12, 55], we conjecture that these three classes of leading singularities suffice to organize the four-point NMHV form factor to *all loop orders* [56].

As a consequence of our conjecture, \mathcal{R}_4 is written as a linear combination of the four cyclic images of R_1 and \bar{R}_1 , together with the two cyclic images of S_1 . At L loops we conjecture that it always admits the decomposition

$$\mathcal{R}_4^{(L)} = \sum_{i=1}^4 \left(R_i f_i^{(L)} + \bar{R}_i \bar{f}_i^{(L)} \right) + \sum_{i=1}^2 S_i f_{s,i}^{(L)}. \quad (5)$$

where R_i , \bar{R}_i and S_i are cyclic images of R_1 , \bar{R}_1 , S_1 respectively, and $f_a^{(L)}$ are weight- $2L$ transcendental functions. Since R_1 and \bar{R}_1 are related by parity, it is natural to introduce the combinations

$$R_1^+ = R_1 + \bar{R}_1, \quad R_1^- = R_1 - \bar{R}_1 \quad (6)$$

together with their cyclic images R_i^+ and R_i^- , $i = 1, \dots, 4$. Equivalently, defining

$$f_{+,1} = \frac{f_1 + \bar{f}_1}{2}, \quad f_{-,1} = \frac{f_1 - \bar{f}_1}{2}, \quad (7)$$

the cyclic ansatz becomes

$$\mathcal{R}_4^{(L)} = \sum_{i=1}^4 \left(R_i^+ f_{+,i}^{(L)} + R_i^- f_{-,i}^{(L)} \right) + \sum_{i=1}^2 S_i f_{s,i}^{(L)}. \quad (8)$$

With this choice, $f_{+,i}^{(L)}$ and $f_{s,i}^{(L)}$ are spacetime parity even, while $f_{-,i}^{(L)}$ is parity odd. We note that the four R_i^- are not independent. Comparing the BCFW representation of the tree-level ratio function with its parity-conjugate representation, denoted P(BCFW), gives the linear relation [57]:

$$R_1^- - R_2^- + R_3^- - R_4^- = 0. \quad (9)$$

Therefore, in a genuine ansatz the redundant odd prefactor should be eliminated, and using (9) the parity-odd part of the ansatz is essentially

$$R_1^- (f_{-,1} + f_{-,4}) + R_2^- (f_{-,2} - f_{-,4}) + R_3^- (f_{-,3} + f_{-,4}). \quad (10)$$

In other words, three special combinations of the four functions $f_{-,i}$ already capture all physical information of the parity-odd part. Finally, the algebraic prefactor S_1 is proportional to the three-mass-triangle square root, so the accompanying function picks up an extra sign when that root changes sign.

Before turning to the explicit bootstrap, we review results at tree-level and one-loop order. At tree level, only one function is present (for $i = 1, 2, 3, 4$),

$$f_{+,i}^{(0)} = \frac{1}{2}, \quad f_{-,i}^{(0)} = f_{s,i}^{(0)} = 0. \quad (11)$$

i.e. the tree-level NMHV form factor is given by the cyclic sum of the parity-even leading singularities alone. At one loop the same organization persists: the parity-odd function is still absent, while the parity-even and algebraic sectors are given by weight-two functions [11, 50],

$$f_{-,i}^{(1)} = 0, \quad f_{+,i}^{(1)} = V_i, \quad f_{s,i}^{(1)} = T_i, \quad (12)$$

where V_i denotes the corresponding finite combination of one one-mass box function and two two-mass-hard box functions [33], while T_i is the corresponding finite three-mass triangle function. At two loops, our goal is to bootstrap the three functions $f_{+,i}^{(2)}$, $f_{-,i}^{(2)}$, and $f_{s,i}^{(2)}$.

TWO-LOOP FUNCTION SPACE

We now specify the function space for the three transcendental functions. Rather than constructing symbols from an alphabet, we start from the known symbol space of two-loop five-point one-mass Feynman integrals [44–47], supplemented by the relevant products of lower-weight functions. For the non-planar sector, we only need

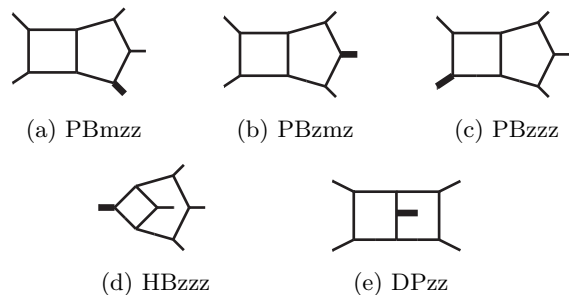


FIG. 2: Two-loop five-point one-mass Feynman integral families for form factor bootstrap.

the topologies in which the non-planar leg is massive, so only the five integral families in Fig. 2 enter the calculation. This is the natural input for the transcendental function basis of the present problem, analogous to previous bootstraps for amplitudes and form factors [32, 58–61]. Collecting the symbols of all these functions gives a space of size 989 with 113 symbol letters. The relevant algebraic dependence involves four square roots

$$\left\{ r_1 = \sqrt{\lambda(u_2, u_4, 1)}, \quad \Sigma_1 = \sqrt{\lambda(u_1 u_4, u_2 u_3, v_1 v_3)} \right\} \quad (13)$$

and their cyclic images $\{r_2, \Sigma_2\}$ with $\lambda(x, y, z) := x^2 + y^2 + z^2 - 2xy - 2xz - 2yz$, together with the parity-odd Lorentz invariant $\text{tr}_5 := 4i\epsilon_{\mu\nu\rho\sigma} p_1^\mu p_2^\nu p_3^\rho p_4^\sigma$. Since we are bootstrapping the ratio function, however, the final answer must be a finite combination of master integrals with all infrared divergences canceled, which reduces the initial space to 638. Combined with the cyclic ansatz, this gives an initial count of $3 \times 638 = 1914$ unknowns. The bootstrap problem is then to determine the unique physical answer within this space.

BOOTSTRAP

To fix the ansatz, we impose various constraints in stages, beginning with intrinsic consistency conditions on the function space and prefactors before turning to physical singularities and limits.

1. Galois and parity symmetry We first impose the Galois-symmetry constraints associated with the algebraic roots, together with ordinary spacetime parity acting through tr_5 . Since the non-planar roots Σ_1, Σ_2 do not appear in the leading singularities, the final answer must be even under their sign flips. By contrast, $S_1 \propto 1/r_2$ requires $f_{s,1}$ to be odd under $r_2 \rightarrow -r_2$, while $f_{\pm,1}$ are even under these root flips. Finally, as mentioned above, under parity $\text{tr}_5 \rightarrow -\text{tr}_5$, $f_{+,1}$ and $f_{s,1}$ are even while $f_{-,1}$ is odd. After imposing these constraints, the ansatz is reduced to 605 unknown coefficients.

2. Dihedral symmetry We then impose the dihedral symmetry of the ansatz, which translates into symmetry properties of the coefficient functions inherited from the

TABLE I: Numbers of unknowns left under successive bootstrap constraints.

| Condition | Unknowns left |
|--------------------------------------|---------------|
| leading singularities and finiteness | 1914 |
| Galois and parity | 605 |
| Dihedral symmetry | 308 |
| Spurious-pole cancellation | 88 |
| Collinear limit $p_4 p_3$ | 7 |
| Triple-collinear $p_4 p_3 p_2$ | 0 |
| Soft limit | 0 |
| Double-soft | 0 |

prefactors. The functions $f_{+,1}$ and $f_{-,1}$ respect the $1 \leftrightarrow 3$ symmetry of R_1 and \bar{R}_1 in Fig. 1, while $f_{s,1}$ obeys the cyclic-by-two symmetry and the reflection $\{1 \leftrightarrow 4, 2 \leftrightarrow 3\}$ of S_1 . After this step, the ansatz is reduced to 308 parameters.

3. Spurious-pole cancellation We next impose spurious-pole cancellation. Up to dihedral symmetry, the form factor R -invariants have a single type of spurious pole, $\langle 3, 4, 1^+, 3^+ \rangle \rightarrow 0$, written in the periodic momentum-twistor notation reviewed in the Supplemental Material. On this locus the unphysical pole in the prefactors must cancel in the full ratio function, leading for example to

$$f_4 - \bar{f}_1 + f_{s,1} \Big|_{\langle 3,4,1^+,3^+ \rangle \rightarrow 0} \rightarrow 0. \quad (14)$$

After imposing this condition, the ansatz has 88 parameters left.

4. Collinear limit We then impose the collinear limit $p_4||p_3$. In this limit only the prefactors \bar{R}_2 , \bar{R}_3 , and S_1 survive, and they all reduce to the three-point NMHV tree prefactor; all other prefactors vanish. Since the three-point NMHV ratio function vanishes at any loop order, the accompanying functions must obey

$$\bar{f}_2 + \bar{f}_3 + f_{s,1} \Big|_{p_4||p_3} \rightarrow 0. \quad (15)$$

This reduces the unknowns in the ansatz to seven.

5. Triple-collinear limit Finally, we impose a triple-collinear consistency condition [62–64] by taking $p_4||p_3||p_2$.

In the triple-collinear limit, the four-point NMHV form factor factorizes into a product of a two-point MHV form factor and the $\mathcal{N} = 4$ triple-collinear splitting function of Grassmann degree four. After normalizing by the corresponding MHV sector, this gives a direct constraint on the ratio function. The same splitting ratio can be extracted from the triple-collinear limit of six-point NMHV amplitudes. In practice, we impose this constraint on

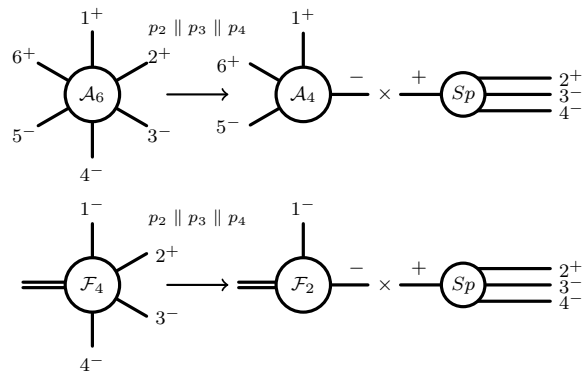


FIG. 3: Triple-collinear matching between the six-point NMHV amplitude and the four-point NMHV form factor on one super-component.

components. This matching is illustrated in Fig. 3. For instance, after extracting $\{+ + - - +\}$ of the six-point amplitude and the $\{- + - -\}$ component of the four-point form factor, in the limit $p_2^+ || p_3^- || p_4^-$ the six-point amplitude and four-point form factor both reduce to the two-loop splitting function ($g^+ g^- g^- \rightarrow g^+$).

We find that, under the triple-collinear limits, the form factor leading singularities and the R -invariants (i), $i = 1, \dots, 6$, of the six-point NMHV amplitudes [65, 66] match each other as

$$\begin{aligned} R_1^\pm &\rightarrow (5) \pm (2), & R_2^\pm &\rightarrow (6) \pm (3), & R_3^\pm &\rightarrow (1) \pm (4), \\ R_4^\pm &\rightarrow 0, & S_1 &\rightarrow (1) + (4), & S_2 &\rightarrow (2) + (5), \end{aligned} \quad (16)$$

regardless of the super-component. Therefore, using the relation $(1) + (3) + (5) = (2) + (4) + (6)$ to solve (6), these matchings imply the following constraints on the ansatz,

$$\begin{aligned} f_{s,1} + f_2 + f_3 &\rightarrow g_1, & f_{s,2} + \bar{f}_1 - f_2 &\rightarrow g_2, \\ f_2 + f_2 &\rightarrow g_3, & f_{s,1} - f_2 + f_3 &\rightarrow g_4, \\ f_{s,2} + f_1 + f_2 &\rightarrow g_5. \end{aligned}$$

Here the g_i are the functions accompanying (i), extracted from the known six-point two-loop NMHV amplitude data [65]. These component matchings remove the seven parameters left after the ordinary collinear limit, so triple-collinear consistency fixes the ansatz completely. A compact summary of the resulting dimension counts is given in Table I.

RESULTS

The bootstrap determines the two-loop four-point NMHV ratio function uniquely at symbol level. The result is specified by the cyclic ansatz in Eq. (8), supplemented by the parity-odd organization in Eq. (10). We provide the symbols for $f_{+,1}^{(2)}$, $f_{s,1}^{(2)}$ and three independent parity-odd combinations in Eq. (10) in the ancillary file NMHVFF2L4pt.m.

The most important independent checks come from soft and double-soft limits. The ratio function vanishes in the soft limit, and it reduces in the double-soft limit to the double soft-gluon current function [67, 68] with helicity (+−) in $\mathcal{N}=4$ sYM, which can also be extracted from NMHV six-point amplitudes. These limits provide sharp validations of the bootstrapped answer and will be important starting points for extracting further physics from the two-loop result.

The final NMHV symbol involves 78 letters. This is already substantially richer than the two-loop MHV case, but all 78 letters still lie inside the 88-letter alphabet that appears for the four-point MHV form factor at higher loop order (missing $a_{27}, \dots, a_{34}, a_{55}, a_{56}$; more details are given in the Supplemental Material). This is one of the main structural lessons of the bootstrap: despite the non-trivial prefactors, including algebraic ones, no new letters are required for two-loop four-point NMHV form factors beyond the 88-letter alphabet known in the MHV sector. This strongly suggests that it is the natural universal alphabet for four-point form factors in planar $\mathcal{N}=4$ sYM.

CONCLUSIONS AND OUTLOOK

We have bootstrapped the planar two-loop NMHV ratio function for the form factor of the chiral stress-tensor supermultiplet in $\mathcal{N}=4$ sYM. This gives the first two-loop result for a non-MHV four-point form factor in planar $\mathcal{N}=4$ sYM and provides direct evidence that the 88-letter function space already known from the MHV sector extends beyond MHV. Our results also satisfy strong consistency conditions, in particular, soft and double-soft limits, as well as collinear and triple-collinear consistency, which provide strong validation. It would be interesting to formulate the splitting functions of the triple-collinear and double-soft limits directly in supersymmetrized form.

It is also highly desirable to further study the potential physical implications of our result for Higgs physics, especially Higgs-to-jet amplitudes in the large-top-mass limit. In particular, it would be interesting to obtain the full function-level result and study its relation to the maximal-weight part of the very recent two-loop Higgs-plus-two-jets results [69], like the generalized maximal-weight principle found in [61]. Other important limits, especially Regge limits [70], multi-particle factorization [71], light-like limit [58], and self-crossing kinematics [72], are also worth investigating, and are expected to yield valuable physical insights into topics such as double parton scattering and BFKL evolution with Higgs production.

Looking further ahead, our result supports the all-loop organization based on leading singularities in Eq. (5). This opens up the exciting prospect of bootstrapping the three-loop and higher-loop four-point NMHV form factor, thereby providing a direct test of this and whether

the same 88-letter alphabet continues to suffice; it could be another “stable” alphabet to all loops in $\mathcal{N}=4$ sYM, in addition to A_3, E_6 for six- and seven-gluon amplitudes and C_2 for three-gluon form factors. Finally, one may ask whether an antipodal duality analogous to the MHV case survives here, which involves only the parity-even part; it would be interesting to understand what object, if any, should be dual to it.

ACKNOWLEDGMENTS

We thank Lance Dixon, Johannes Henn and Zhenjie Li for inspiring discussions, and Lance Dixon, Johannes Henn and Gang Yang for helpful comments on the draft. S.H. is supported by the National Natural Science Foundation of China under Grant No. 12225510, 12447101, and by the New Cornerstone Science Foundation. Q.Y. is supported by the European Union (ERC, UNIVERSE PLUS, 101118787). Views and opinions expressed are however those of the authors only and do not necessarily reflect those of the European Union or the European Research Council Executive Agency. Neither the European Union nor the granting authority can be held responsible for them. J.L. thanks the Max Planck Institute for Physics for its hospitality during the course of this work.

* songhe@itp.ac.cn

† liujiahao@itp.ac.cn

‡ qlyang@mpp.mpg.de

- [1] F. Wilczek, Phys. Rev. Lett. **39**, 1304 (1977).
- [2] M. A. Shifman, A. I. Vainshtein, and V. I. Zakharov, Phys. Lett. B **78**, 443 (1978).
- [3] W. L. van Neerven, Z. Phys. C **30**, 595 (1986).
- [4] N. Arkani-Hamed, L. J. Dixon, A. J. McLeod, M. Spradlin, J. Trnka, and A. Volovich, Snowmass 2021 (2022), arXiv:2207.10636 [hep-th].
- [5] J. Maldacena and A. Zhiboedov, JHEP **11**, 104, arXiv:1009.1139 [hep-th].
- [6] L. F. Alday and J. Maldacena, JHEP **11**, 068, arXiv:0710.1060 [hep-th].
- [7] A. Brandhuber, B. Spence, G. Travaglini, and G. Yang, JHEP **01**, 134, arXiv:1011.1899 [hep-th].
- [8] A. Brandhuber, O. Gürdoğan, R. Mooney, G. Travaglini, and G. Yang, JHEP **10**, 046, arXiv:1107.5067 [hep-th].
- [9] Z. Gao and G. Yang, JHEP **06**, 105, arXiv:1303.2668 [hep-th].
- [10] Z. Li, JHEP **05**, 209, arXiv:2412.17974 [hep-th].
- [11] L. Bianchi, A. Brandhuber, R. Panerai, and G. Travaglini, JHEP **02**, 182, arXiv:1812.09001 [hep-th].
- [12] R. Frassek, D. Meidinger, D. Nandan, and M. Wilhelm, JHEP **01**, 182, arXiv:1506.08192 [hep-th].
- [13] L. V. Bork and A. I. Onishchenko, JHEP **12**, 076, arXiv:1607.00503 [hep-th].
- [14] L. V. Bork and A. I. Onishchenko, JHEP **04**, 019, arXiv:1607.02320 [hep-th].

- [15] R. H. Boels, B. A. Kniehl, O. V. Tarasov, and G. Yang, *JHEP* **02**, 063, arXiv:1211.7028 [hep-th].
- [16] G. Yang, *Phys. Rev. Lett.* **117**, 271602 (2016), arXiv:1610.02394 [hep-th].
- [17] G. Lin, G. Yang, and S. Zhang, *Phys. Rev. Lett.* **127**, 171602 (2021), arXiv:2106.05280 [hep-th].
- [18] G. Lin, G. Yang, and S. Zhang, *Sci. China Phys. Mech. Astron.* **67**, 241011 (2024), arXiv:2112.09123 [hep-th].
- [19] A. Sever, A. G. Tumanov, and M. Wilhelm, *Phys. Rev. Lett.* **126**, 031602 (2021), arXiv:2009.11297 [hep-th].
- [20] A. Sever, A. G. Tumanov, and M. Wilhelm, *JHEP* **10**, 071, arXiv:2105.13367 [hep-th].
- [21] A. Sever, A. G. Tumanov, and M. Wilhelm, *JHEP* **03**, 128, arXiv:2112.10569 [hep-th].
- [22] B. Basso and A. G. Tumanov, *JHEP* **02**, 022, arXiv:2308.08432 [hep-th].
- [23] S. Caron-Huot, L. J. Dixon, J. M. Drummond, F. Dulat, J. Foster, Ö. Gürdoğan, M. von Hippel, A. J. McLeod, and G. Papathanasiou, *PoS CORFU2019*, 003 (2020), arXiv:2005.06735 [hep-th].
- [24] L. J. Dixon, A. J. McLeod, and M. Wilhelm, *JHEP* **04**, 147, arXiv:2012.12286 [hep-th].
- [25] L. J. Dixon, Ö. Gürdoğan, Y.-T. Liu, A. J. McLeod, and M. Wilhelm, *Phys. Rev. Lett.* **130**, 111601 (2023), arXiv:2212.02410 [hep-th].
- [26] L. J. Dixon, O. Gürdoğan, A. J. McLeod, and M. Wilhelm, *JHEP* **07**, 153, arXiv:2204.11901 [hep-th].
- [27] L. J. Dixon and S. Xin, *JHEP* **01**, 012, [Erratum: *JHEP* **03**, 159 (2026)], arXiv:2411.01571 [hep-th].
- [28] Y. Guo, L. Wang, G. Yang, and Y. Yin, *JHEP* **02**, 002, arXiv:2409.12445 [hep-th].
- [29] L. Dixon and Z. Li, To appear.
- [30] B. Basso, L. J. Dixon, and A. G. Tumanov, *JHEP* **02**, 034, arXiv:2410.22402 [hep-th].
- [31] J. M. Henn, J. Lim, and W. J. Torres Bobadilla, *JHEP* **02**, 085, arXiv:2410.22465 [hep-th].
- [32] Y. Guo, L. Wang, and G. Yang, *Phys. Rev. Lett.* **127**, 151602 (2021), arXiv:2106.01374 [hep-th].
- [33] L. Bianchi, A. Brandhuber, R. Panerai, and G. Travaglini, *JHEP* **02**, 134, arXiv:1812.10468 [hep-th].
- [34] L. J. Dixon, O. Gürdoğan, A. J. McLeod, and M. Wilhelm, *Phys. Rev. Lett.* **128**, 111602 (2022), arXiv:2112.06243 [hep-th].
- [35] L. J. Dixon and Y.-T. Liu, *JHEP* **09**, 098, arXiv:2308.08199 [hep-th].
- [36] A. Brandhuber, G. Travaglini, and G. Yang, *JHEP* **05**, 082, arXiv:1201.4170 [hep-th].
- [37] C. Duhr, *JHEP* **08**, 043, arXiv:1203.0454 [hep-ph].
- [38] X. Chen, X. Guan, and B. Mistlberger, (2025), arXiv:2504.06490 [hep-ph].
- [39] A. V. Kotikov and L. N. Lipatov, *Nucl. Phys. B* **661**, 19 (2003), [Erratum: *Nucl.Phys.B* 685, 405–407 (2004)], arXiv:hep-ph/0208220.
- [40] A. V. Kotikov, L. N. Lipatov, A. I. Onishchenko, and V. N. Velizhanin, *Phys. Lett. B* **595**, 521 (2004), [Erratum: *Phys.Lett.B* 632, 754–756 (2006)], arXiv:hep-th/0404092.
- [41] L. J. Dixon, *JHEP* **01**, 075, arXiv:1712.07274 [hep-th].
- [42] A. B. Goncharov, M. Spradlin, C. Vergu, and A. Volovich, *Phys. Rev. Lett.* **105**, 151605 (2010), arXiv:1006.5703 [hep-th].
- [43] C. Duhr, H. Gangl, and J. R. Rhodes, *JHEP* **10**, 075, arXiv:1110.0458 [math-ph].
- [44] S. Abreu, H. Ita, F. Moriello, B. Page, W. Tschernow, and M. Zeng, *JHEP* **11**, 117, arXiv:2005.04195 [hep-ph].
- [45] D. Chicherin, V. Sotnikov, and S. Zoia, *JHEP* **01**, 096, arXiv:2110.10111 [hep-ph].
- [46] S. Abreu, H. Ita, B. Page, and W. Tschernow, *JHEP* **03**, 182, arXiv:2107.14180 [hep-ph].
- [47] S. Abreu, D. Chicherin, H. Ita, B. Page, V. Sotnikov, W. Tschernow, and S. Zoia, *Phys. Rev. Lett.* **132**, 141601 (2024), arXiv:2306.15431 [hep-ph].
- [48] J. M. Henn, *Phys. Rev. Lett.* **110**, 251601 (2013), arXiv:1304.1806 [hep-th].
- [49] J. M. Henn, *J. Phys. A* **48**, 153001 (2015), arXiv:1412.2296 [hep-ph].
- [50] L. V. Bork, *JHEP* **01**, 049, arXiv:1203.2596 [hep-th].
- [51] L. V. Bork, D. I. Kazakov, and G. S. Vartanov, *JHEP* **10**, 133, arXiv:1107.5551 [hep-th].
- [52] J. M. Drummond, J. Henn, G. P. Korchemsky, and E. Sokatchev, *Nucl. Phys. B* **828**, 317 (2010), arXiv:0807.1095 [hep-th].
- [53] F. Cachazo, (2008), arXiv:0803.1988 [hep-th].
- [54] M. Bullimore, L. J. Mason, and D. Skinner, *JHEP* **03**, 070, arXiv:0912.0539 [hep-th].
- [55] N. Arkani-Hamed, J. L. Bourjaily, F. Cachazo, A. B. Goncharov, A. Postnikov, and J. Trnka, *Grassmannian Geometry of Scattering Amplitudes* (Cambridge University Press, 2016) arXiv:1212.5605 [hep-th].
- [56] We note that the leading singularities of the form factor at all-loop orders, along with their corresponding on-shell diagrams, can always be obtained from the one-loop leading singularity through gluing operations, including BCFW bridges and inverse-soft factors [55]. Similar to the case of scattering amplitudes, these operations do not introduce additional R-invariants beyond one-loop leading singularities. We therefore propose this hypothesis. In subsequent calculations, once a unique solution is obtained via the bootstrap approach, this conjecture will be fully verified at two loops.
- [57] L. V. Bork, *JHEP* **12**, 111, arXiv:1407.5568 [hep-th].
- [58] Y. Guo, L. Wang, and G. Yang, *Commun. Theor. Phys.* **77**, 055203 (2025), arXiv:2209.06816 [hep-th].
- [59] S. Carròlo, D. Chicherin, J. Henn, Q. Yang, and Y. Zhang, *JHEP* **07**, 214, arXiv:2505.01245 [hep-th].
- [60] S. Carròlo, D. Chicherin, J. Henn, Q. Yang, and Y. Zhang, *Phys. Rev. Lett.* **136**, 181602 (2026), arXiv:2510.20565 [hep-th].
- [61] S. Carròlo, D. Chicherin, J. Henn, Q. Yang, and Y. Zhang, (2026), arXiv:2602.02783 [hep-th].
- [62] S. Catani and M. Grazzini, *Phys. Lett. B* **446**, 143 (1999), arXiv:hep-ph/9810389.
- [63] S. Catani, D. de Florian, and G. Rodrigo, *Phys. Lett. B* **586**, 323 (2004), arXiv:hep-ph/0312067.
- [64] S. Badger, F. Buciumi, and T. Peraro, *JHEP* **09**, 188, arXiv:1507.05070 [hep-ph].
- [65] D. A. Kosower, R. Roiban, and C. Vergu, *Phys. Rev. D* **83**, 065018 (2011), arXiv:1009.1376 [hep-th].
- [66] L. J. Dixon, J. M. Drummond, and J. M. Henn, *JHEP* **01**, 024, arXiv:1111.1704 [hep-th].
- [67] Y. J. Zhu, *JHEP* **02**, 018, arXiv:2009.08919 [hep-ph].
- [68] M. Czakon, F. Eschment, and T. Schellenberger, *JHEP* **04**, 065, arXiv:2211.06465 [hep-ph].
- [69] G. De Laurentis, H. Ita, V. Kuschke, M. Ruf, and V. Sotnikov, (2026), arXiv:2605.04009 [hep-ph].
- [70] V. Del Duca and L. J. Dixon, *J. Phys. A* **55**, 443016 (2022), arXiv:2203.13026 [hep-th].

- [71] L. J. Dixon and M. von Hippel, JHEP **10**, 065, arXiv:1408.1505 [hep-th].
- [72] L. J. Dixon and I. Esterlis, JHEP **07**, 116, [Erratum: JHEP 08, 131 (2016)], arXiv:1602.02107 [hep-th].
- [73] A. Hodges, JHEP **05**, 135, arXiv:0905.1473 [hep-th].
- [74] N. Arkani-Hamed, J. L. Bourjaily, F. Cachazo, and J. Trnka, JHEP **06**, 125, arXiv:1012.6032 [hep-th].
- [75] L. F. Alday, D. Gaiotto, J. Maldacena, A. Sever, and P. Vieira, JHEP **04**, 088, arXiv:1006.2788 [hep-th].
- [76] V. P. Nair, Phys. Lett. B **214**, 215 (1988).

Supplemental Material

PERIODIC MOMENTUM TWISTORS AND OPE PARAMETRIZATIONS

Momentum twistors [73] are natural variables for lightlike dual contours (see also [74]): a cusp x_i is represented by the line (Z_{i-1}, Z_i) , while dual-conformal quantities can be written in terms of homogeneous four-brackets. For form factors, the nonzero operator momentum q makes the dual lightlike contour open after one pass through the external particles; the contour is instead arranged periodically, with neighboring periods shifted by q . This is the periodic Wilson-loop picture of form factor kinematics [5, 7, 9], which we now adapt to the four-point case considered in the main text. For the four-point case, we use dual coordinates

$$p_i = x_{i+1} - x_i, \quad q = \sum_{i=1}^4 p_i, \quad i = 1, \dots, 4. \quad (\text{S1})$$

Since $q \neq 0$, these dual points do not form a closed polygon. Following the periodic prescription for form factors, we have $x_{i+4} = x_i + q$. Shifted labels such as $i+4$ therefore denote image points rather than labels reduced modulo four; for the corresponding spinors we take $\lambda_{i+4} = \lambda_i$.

The momentum twistors are

$$Z_i = (\lambda_i^\alpha, \mu_i^{\dot{\alpha}}), \quad \mu_i^{\dot{\alpha}} = x_i^{\alpha\dot{\alpha}} \lambda_{i\alpha} = x_{i+1}^{\alpha\dot{\alpha}} \lambda_{i\alpha}. \quad (\text{S2})$$

For compactness we denote the images under one positive or negative period by

$$Z_i^+ \equiv Z_{i+4}, \quad Z_i^- \equiv Z_{i-4}. \quad (\text{S3})$$

Thus Z_i^+ has the same spinor part as Z_i but μ_i shifted by $q\lambda_i$. We write four-brackets as $\langle ijkl \rangle = \det(Z_i, Z_j, Z_k, Z_l)$. We also introduce the infinity twistor, which projects a pair of momentum twistors onto the ordinary spinor bracket. With $Z^{\hat{A}} = (\lambda^\alpha, \mu^{\dot{\alpha}})$, we use

$$(I_\infty)_{\hat{A}\hat{B}} = \begin{pmatrix} \epsilon_{\alpha\beta} & 0 \\ 0 & 0 \end{pmatrix}, \quad \langle ij \rangle = (I_\infty)_{\hat{A}\hat{B}} Z_i^{\hat{A}} Z_j^{\hat{B}} = \epsilon_{\alpha\beta} \lambda_i^\alpha \lambda_j^\beta. \quad (\text{S4})$$

The standard relation between dual distances and four-brackets is $x_{ij}^2 = \langle i-1 \ i \ j-1 \ j \rangle / (\langle i-1 \ i \rangle \langle j-1 \ j \rangle)$, where $\langle ij \rangle$ is the usual spinor bracket. The variables used in the main text can therefore be represented as $u_i = x_{i,i+2}^2 / x_{i,i+4}^2$ and $v_i = x_{i,i+3}^2 / x_{i,i+4}^2$, or equivalently $u_i = \langle i-1 \ i \ i+1 \ i+2 \rangle \langle i+3 \ i+4 \rangle / (\langle i-1 \ i \ i+3 \ i+4 \rangle \langle i+1 \ i+2 \rangle)$ and $v_i = \langle i-1 \ i \ i+2 \ i+3 \rangle \langle i+3 \ i+4 \rangle / (\langle i-1 \ i \ i+3 \ i+4 \rangle \langle i+2 \ i+3 \rangle)$. Here and below, the shifted labels are interpreted using the periodic contour.

We also use an OPE parametrization of the periodic momentum twistors. The variables T_a, S_a, F_a are those of the Wilson-loop OPE [75] and its form factor extensions [19–22]; we follow the explicit four-point parametrization of Ref. [10]. The transition between neighboring periods is

$$Z_{i+4} = P Z_i, \quad (\text{S5})$$

with

$$P = \begin{pmatrix} 2 & 1 & 0 & 0 \\ -1 & 0 & 0 & 0 \\ 0 & 0 & 2 & 1 \\ 0 & 0 & -1 & 0 \end{pmatrix}. \quad (\text{S6})$$

The twistors in one period are parametrized as

$$\begin{aligned} Z_1 &= M_1(0, 1, 0, 1)^\top, & Z_2 &= M_1 M_2(1, 3, -1, 1)^\top, \\ Z_3 &= M_1 M_2(1, 1, -2, 0)^\top, & Z_4 &= (0, 0, 1, 0)^\top, \end{aligned} \quad (\text{S7})$$

where

$$M_1 = \begin{pmatrix} T_1 & 0 & 0 & 0 \\ 0 & T_1^{-1} & 0 & 0 \\ 0 & 0 & S_1 & 0 \\ 0 & 0 & 0 & S_1^{-1} \end{pmatrix}, \quad (\text{S8})$$

and

$$M_2 = \frac{1}{\sqrt{F_2 S_2 T_2}} \begin{pmatrix} F_2 S_2 & 0 & 0 & 0 \\ -F_2 S_2 (T_2^2 - 1) & F_2 S_2 T_2^2 & 0 & S_2 T_2 (S_2 - F_2 T_2) \\ T_2 - F_2 S_2 & 0 & T_2 & 0 \\ 0 & 0 & 0 & S_2^2 T_2 \end{pmatrix}. \quad (\text{S9})$$

In this explicit OPE frame, following Ref. [10], the infinity twistor is represented as the bi-twistor

$$I_\infty^{\text{OPE}} = \begin{pmatrix} 1 & -1 & 0 & 0 \\ 0 & 0 & 1 & -1 \end{pmatrix}^\top, \quad \langle ij \rangle = \langle ij I_\infty^{\text{OPE}} \rangle. \quad (\text{S10})$$

Here $\langle ij I_\infty^{\text{OPE}} \rangle$ denotes the four-bracket formed from Z_i, Z_j and the two columns of I_∞^{OPE} . This choice is adapted to the transition matrix because $\text{PI}_\infty^{\text{OPE}} = I_\infty^{\text{OPE}}$. Any dual conformal ratio can be obtained from the four-brackets of the twistors in Eqs. (S5)–(S9), while spinor brackets are evaluated using Eq. (S10).

FORM FACTOR R-INVARIANTS

Here we collect the form factor leading singularities that enter the ansatz (8). We use the standard on-shell superspace variables η_i^A , $A = 1, \dots, 4$ [76]. For form factors of the stress-tensor multiplet, one also introduces the Grassmann momentum $\gamma^{A\alpha}$ carried by the operator insertion [8]. The dual Grassmann coordinates are defined by

$$\theta_{i+1}^{A\alpha} - \theta_i^{A\alpha} = \lambda_i^\alpha \eta_i^A, \quad \gamma^{A\alpha} = \sum_{i=1}^4 \lambda_i^\alpha \eta_i^A. \quad (\text{S11})$$

In parallel, they obey $\theta_{i+4}^{A\alpha} = \theta_i^{A\alpha} + \gamma^{A\alpha}$. The corresponding supertwistors are

$$\mathcal{Z}_i = (Z_i, \chi_i), \quad \chi_i^A = \theta_i^{A\alpha} \lambda_{i\alpha}, \quad \chi_i^\pm \equiv \chi_{i\pm 4}. \quad (\text{S12})$$

The basic NMHV building block is the five-bracket

$$[a, b, c, d, e] = \frac{\delta^{(4)}(\chi_a \langle bcde \rangle + \chi_b \langle cdea \rangle + \chi_c \langle deab \rangle + \chi_d \langle eabc \rangle + \chi_e \langle abcd \rangle)}{\langle abcd \rangle \langle bcde \rangle \langle cdea \rangle \langle deab \rangle \langle eabc \rangle}. \quad (\text{S13})$$

Here the Grassmann delta function is understood as

$$\delta^{(4)}(\Xi) = \Xi^1 \Xi^2 \Xi^3 \Xi^4, \quad \Xi^A = \chi_a^A \langle bcde \rangle + \chi_b^A \langle cdea \rangle + \chi_c^A \langle deab \rangle + \chi_d^A \langle eabc \rangle + \chi_e^A \langle abcd \rangle. \quad (\text{S14})$$

Since each χ_i^A is linear in the on-shell variables η_j^A , this numerator is a homogeneous degree-four polynomial in the η 's, as appropriate for an NMHV invariant. For six-point NMHV amplitude, we denote (1) := [23456] and so on, where the six R -invariants satisfy (1) + (3) + (5) = (2) + (4) + (6).

For form factors, the five-brackets involve periodic supertwistors introduced in the previous section. Shifted labels are written as i^\pm as in Eq. (S3). There are two generic on-shell configurations,

$$R'_{rst} = \begin{array}{c} \begin{array}{ccccc} & s-1 & s & t-1 & \\ & \circ & \circ & & \\ \vdots & \vdots & \vdots & & \\ r+1 & \circ & \circ & & \\ & \vdots & \vdots & & \\ & \circ & \circ & & \\ & r & r-1 & & \end{array} \\ \end{array}, \quad R''_{rst} = \begin{array}{c} \begin{array}{ccccc} & s-1 & s & t-1 & \\ & \circ & \circ & & \\ \vdots & \vdots & \vdots & & \\ r+1 & \circ & \circ & & \\ & \vdots & \vdots & & \\ & \circ & \circ & & \\ & r & r-1 & & \end{array} \\ \end{array}. \quad (\text{S15})$$

For $s \neq t$, these two placements of the operator insertion give the same periodic momentum-twistor invariant after the corresponding region-variable assignment. In the notation used in the main text, we suppress the primes and write

$$R_{rst} \equiv R'_{rst} = R''_{rst} = [s-1, s, t-1, t, r]. \quad (\text{S16})$$

The boundary case of the first configuration is also needed for the four-point NMHV form factor. Here the operator sits at a three-point corner, and the corresponding invariant is

$$R'_{rss} = \begin{array}{c} \begin{array}{c} s-1 \\ \circ \\ \vdots \\ r+1 \end{array} \\ \begin{array}{c} \circ \\ \vdots \\ r \end{array} \\ \begin{array}{c} \circ \\ \vdots \\ r-1 \end{array} \end{array} = \frac{\langle r (s-1)^- s^- s \rangle \langle r s-1 s (s-1)^- \rangle}{\langle r^+ s-1 s r \rangle \langle s s^- s-1 (s-1)^- \rangle} [(s-1)^-, s^-, s-1, s, r]. \quad (\text{S17})$$

In our notation, this boundary invariant is denoted simply by $R_{rss} \equiv R'_{rss}$.

The two prefactors used in the main text are obtained from Eqs. (S16) and (S17). The non-boundary representative is

$$R_{241} = \begin{array}{c} \begin{array}{c} 2 \\ \circ \\ \vdots \\ 1 \end{array} \\ \begin{array}{c} \circ \\ \vdots \\ 1 \end{array} \\ \begin{array}{c} \bullet \\ \vdots \\ 1 \end{array} \end{array} = [2, 3, 4, 4^-, 1]. \quad (\text{S18})$$

The boundary representative is

$$R_{144} = \begin{array}{c} \begin{array}{c} 1 \\ \circ \\ \vdots \\ 1 \end{array} \\ \begin{array}{c} \circ \\ \vdots \\ 1 \end{array} \\ \begin{array}{c} \bullet \\ \vdots \\ 1 \end{array} \end{array} = \frac{\langle 1 3^- 4^- 4 \rangle \langle 1 3 4 3^- \rangle}{\langle 1^+ 3 4 1 \rangle \langle 4 4^- 3 3^- \rangle} [3^-, 4^-, 3, 4, 1] = \begin{array}{c} \begin{array}{c} 2 \\ \bullet \\ \vdots \\ 1 \end{array} \\ \begin{array}{c} \circ \\ \vdots \\ 1 \end{array} \\ \begin{array}{c} \bullet \\ \vdots \\ 1 \end{array} \end{array}, \quad (\text{S19})$$

Thus, R_{144} is the parity conjugate of R_{241} ; this relation becomes manifest after replacing R_{144} by the equivalent on-shell diagram in the last equality [33].

The remaining prefactor in (8), denoted as $S_1 = R_{12,34}$ in the main text, is the algebraic leading singularity associated with the finite three-mass triangle in the four-point NMHV one-loop form factor. Following Ref. [33],

$$R_{12,34} = \begin{array}{c} \begin{array}{c} 1 \\ \circ \\ \vdots \\ 1 \end{array} \\ \begin{array}{c} \circ \\ \vdots \\ 1 \end{array} \\ \begin{array}{c} \circ \\ \vdots \\ 1 \end{array} \end{array} = \frac{1}{2} (\mathcal{L}_{1,3}(\ell^*) + \mathcal{L}_{1,3}(\bar{\ell}^*)) \frac{\sqrt{u_1 u_3}}{r_2}, \quad (\text{S20})$$

where

$$\mathcal{L}_{r,s}(\ell) = [\ell, r, r-1, r^-, (r-1)^-] \times \frac{\langle \ell r r-1 r^- \rangle \langle \ell r^- (r-1)^- r-1 \rangle}{\langle \ell r r-1 s-1 \rangle \langle \ell r^- (r-1)^- s \rangle} \times \frac{\langle s-1 s r-1 r \rangle^{1/2} \langle s-1 s (r-1)^- r^- \rangle^{1/2}}{\langle r-1 r (r-1)^- r^- \rangle}, \quad (\text{S21})$$

and ℓ^* and $\bar{\ell}^*$ are the two solutions of the following cut equations:

$$\langle \ell 4^- 1 \rangle = \langle \ell 2 3 \rangle = \langle \ell 4 1^+ \rangle = \langle \ell I_\infty \rangle = 0. \quad (\text{S22})$$

The individual solutions contain square-root dependence. In the symmetric combination in Eq. (S20), this dependence reduces to a single overall square root, carried by r_2 , in $R_{12,34}$.

SYMBOL ALPHABET OF 88 LETTERS

The four-point MHV form factor has recently been bootstrapped through four loops [29]. In the notation of the ancillary file `aAlphabet.m` of [27], which contains a 93-letter alphabet, all available MHV results through four loops involve only an 88-letter subset. This suggests that the 88-letter subset is a stable alphabet for the four-point form factor. We have also rewritten our NMHV result in the same notation, see `NMHVFF2L4pt_aAlphabet.m`.

This subset is obtained from the 93-letter list by removing five letters: $\{a_{43}, a_{44}, a_{73}, a_{76}, a_{87}\}$. Here we list this 88-letter subset using cyclically independent seeds; all cyclic images are understood. It consists of 68 rational letters and 20 algebraic letters. The rational letters can be written in terms of four-brackets of periodic momentum twistors. The cyclically independent rational seeds are

$$\begin{aligned}
& \langle 1234 \rangle, \langle 1241^+ \rangle, \langle 121^+2^+ \rangle, \langle 1231^+ \rangle, \langle 1232^+ \rangle, \langle 1233^+ \rangle, \langle 1242^+ \rangle, \langle 1343^+ \rangle, \langle 131^+3^+ \rangle, \\
& \langle (1^+2^+) \cap (123) 3^+ 4^+ 1^{++} \rangle, \langle 3^+4^+ (234) \cap (41^+2^+) \rangle, \\
& \langle (41^+) \cap (2^+3^+4^+) 2 (4^+1^{++}) \cap (2^{++}3^{++}4^{++}) 2^+ \rangle, \\
& \langle 1 (23) \cap (41^+2^+) 1^+ (2^+3^+) \cap (4^+1^{++}2^{++}) \rangle, \langle (41^+) \cap (123) 2 (4^+1^{++}) \cap (1^+2^+3^+) 2^+ \rangle, \\
& \langle (12) \cap (1^+2^+3^+) 3 4 2^+ \rangle, \langle (23) \cap (41^+2^+) 2^+ 3^+ 1^{++} \rangle, \langle (41^+) \cap (123) 2 2^+ 3^+ \rangle, \langle (41^+) \cap (123) 2^+ 4^+ 1^{++} \rangle.
\end{aligned} \tag{S23}$$

Some of these rational letters contain intersections of lines and planes in twistor space. Here (ab) denotes the line through Z_a and Z_b , while (abc) denotes the plane through Z_a, Z_b, Z_c . Then \cap denotes the projective intersection: $(ab) \cap (cde)$ is the twistor where the line (ab) meets the plane (cde) , and $(abc) \cap (def)$ is the line common to two planes. These are composite twistors built from the external kinematics. For example,

$$(ab) \cap (cde) = Z_a \langle bcde \rangle - Z_b \langle acde \rangle, \tag{S24}$$

and the corresponding four-brackets can be expanded as

$$\begin{aligned}
\langle (ab) \cap (cde) fgh \rangle &= \langle afgh \rangle \langle bcde \rangle - \langle b f g h \rangle \langle acde \rangle, \\
\langle a b (cde) \cap (fgh) \rangle &= \langle acde \rangle \langle b f g h \rangle - \langle bcde \rangle \langle a f g h \rangle.
\end{aligned} \tag{S25}$$

The algebraic letters involve two cyclically independent square roots, denoted by r_1 and Σ_1 . For each root there are five algebraic seed letters; after including cyclic images these give the remaining 20 letters,

$$\begin{aligned}
r_1 : & \frac{v_1 + v_2 + r_1}{v_1 + v_2 - r_1}, \frac{2 - v_1 - v_2 + r_1}{2 - v_1 - v_2 - r_1}, \frac{v_1 - v_2 + r_1}{v_1 - v_2 - r_1}, \frac{v_1 - v_2 - 2u_1 + 2u_3 + r_1}{v_1 - v_2 - 2u_1 + 2u_3 - r_1}, \frac{P_1 + r_1 \text{tr}_5}{P_1 - r_1 \text{tr}_5} \\
\Sigma_1 : & \frac{u_3 v_1 - u_1 v_2 + u_1 + u_1 u_2 - u_2 u_3 - v_1 + v_1 v_2 + \Sigma_1}{u_3 v_1 - u_1 v_2 + u_1 + u_1 u_2 - u_2 u_3 - v_1 + v_1 v_2 - \Sigma_1}, \\
& \frac{-2u_1 v_1 - 2u_2 v_1 + u_3 v_1 - u_1 v_2 + u_1 + u_1 u_2 - u_2 u_3 + 2v_1^2 + v_2 v_1 - v_1 + \Sigma_1}{-2u_1 v_1 - 2u_2 v_1 + u_3 v_1 - u_1 v_2 + u_1 + u_1 u_2 - u_2 u_3 + 2v_1^2 + v_2 v_1 - v_1 - \Sigma_1}, \\
& \frac{-u_3 v_1 - u_1 v_2 - 2u_2 v_2 + u_1 - u_1 u_2 + 2u_2 + u_2 u_3 - v_1 + v_1 v_2 + \Sigma_1}{-u_3 v_1 - u_1 v_2 - 2u_2 v_2 + u_1 - u_1 u_2 + 2u_2 + u_2 u_3 - v_1 + v_1 v_2 - \Sigma_1}, \\
& \frac{2u_1 v_1 - u_1 v_2 - u_3 v_1 - 2u_1^2 - u_2 u_1 + 2u_3 u_1 + u_1 + u_2 u_3 - v_1 + v_1 v_2 + \Sigma_1}{2u_1 v_1 - u_1 v_2 - u_3 v_1 - 2u_1^2 - u_2 u_1 + 2u_3 u_1 + u_1 + u_2 u_3 - v_1 + v_1 v_2 - \Sigma_1}, \frac{P_2 + \Sigma_1 \text{tr}_5}{P_2 - \Sigma_1 \text{tr}_5},
\end{aligned} \tag{S26}$$

where

$$\begin{aligned}
P_1 &= -u_1 u_2 v_1 + u_3 u_2 v_1 - u_2 v_1 + u_1 u_2 v_2 - u_3 u_2 v_2 - 2u_2 v_1 v_2 - u_2 v_2 - u_3 v_1^2 \\
&\quad - u_1 v_2^2 - u_1 v_1 v_2 - u_3 v_1 v_2 + 2u_2^2 + 2u_1 u_2 + 2u_3 u_2 + v_1 v_2^2 + v_1^2 v_2,
\end{aligned} \tag{S27}$$

and

$$\begin{aligned}
P_2 &= -u_1^2 v_2^2 + 2u_2 u_1^2 v_2 + u_1^2 v_2 + 2u_1 v_1 v_2^2 + u_2 u_1 v_1 - 2u_2 u_3 u_1 v_1 \\
&\quad + u_3 u_1 v_1 - u_2 u_1 v_2 - 2u_2 u_3 u_1 v_2 - 2u_2 u_1 v_1 v_2 - 2u_3 u_1 v_1 v_2 - 2u_1 v_1 v_2 - u_3^2 v_1^2 \\
&\quad - u_3 v_1^2 + 2u_2 u_3^2 v_1 - u_2 v_1 + 2u_3 v_1^2 v_2 + u_2 v_1 v_2 - 2u_2 u_3 v_1 v_2 - u_2^2 u_1^2 \\
&\quad - u_2 u_1^2 + u_2^2 u_1 + u_2 u_1 + 2u_2^2 u_3 u_1 + 3u_2 u_3 u_1 - u_2^2 u_3^2 + u_2^2 u_3 - v_1^2 v_2^2 + v_1^2 v_2.
\end{aligned} \tag{S28}$$

The two-loop NMHV result contains only 78 of these 88 letters, which contains the two-loop MHV alphabet as a subset. The letters absent from the two-loop result are $\{a_{27}, a_{28}, \dots, a_{34}, a_{55}, a_{56}\}$. Here $a_{55} = \Sigma_1^2$ and $a_{56} = \Sigma_2^2$ are the two ‘‘square-root’’ letters mentioned in the main text.